Comparative evaluation of three infiltration models for runoff and erosion prediction in the Loess Plateau region of China

Zhuo Cheng, Bofu Yu, Suhua Fu and Gang Liu

ABSTRACT

Loess Plateau is known for its high rate of soil erosion. Infiltration models are needed to simulate runoff hydrograph for erosion prediction. Rainfall-runoff data at 1-min interval for 33 plot-events in Tuanshangou catchment were used to evaluate three infiltration models: constant infiltration (CI) rate, spatially variable infiltration (VI) rate, and Green–Ampt (GA). Each of the three models has three parameters. The three models performed similarly when calibrated for individual storms with a Nash–Sutcliffe coefficient (NSC) of efficiency of around 0.76, with better performance for large storm events. For all three models, the total runoff amount is well simulated while the modelled peak runoff rate is systematically smaller by about 30%. The variation in the initial infiltration amount is smaller than that in other infiltration parameters. For ungauged events, averaged parameter values were used to predict runoff hydrographs, and the results showed a decrease in model performance with the average NSC reduced to 0.47. One advantage in using the spatially VI model is that the simulated runoff is least sensitive to changes in model parameters compared with the other two models, as a 10% variation in parameter values would lead to 5% variations on average in the simulated runoff for VI, while around 8.6% for the other two.

Key words | comparison, infiltration, Loess Plateau, modelling

Zhuo Cheng
Gang Liu
State Key Laboratory of Earth Surface Processes and Resource Ecology,
Beijing Normal University,
Beijing 100875, China

Bofu Yu (corresponding author)
Australian Rivers Institute and School of Engineering,
Griffith University,
Nathan 4111, Australia
E-mail: *b.yu@griffith.edu.au*

Suhua Fu
State Key Laboratory of Soil Erosion and Dryland Farming on the Loess Plateau,
Institute of Soil and Water Conservation, Chinese Academy of Sciences,
Yangling, Shaanxi 712100, China
and
Faculty of Geographical Science,
Beijing Normal University,
Beijing 100875, China

INTRODUCTION

Water erosion is one of the fundamental earth surficial processes and one of the well acknowledged environmental issues because of its on-site impact on agricultural production and off-site impact on water quality. For water and soil conservation, models have been developed to predict the rate of soil loss as a function of climate, topography, soil, vegetation cover and management practices, e.g. the Universal Soil Loss Equation (USLE) (Wischmeier & Smith 1978). More recently, attempts have been made to develop and test water erosion prediction technologies based on our understanding of the underlying biophysical processes of erosion. Common to all these process-based erosion models is a necessary component to describe runoff generation processes and to predict hydrographs. Runoff plays a dual role in erosion processes. First, runoff detaches the soil, in the form of primary particles and aggregates, from the soil matrix, especially on steep slopes, and subsequently runoff carries eroded sediments into gullies and streams. For instance, in WEPP (Water Erosion Prediction Project) (Nearing *et al.* 1989; Foster *et al.* 1995), the Green–Ampt (GA) infiltration model (Green & Ampt 1911) was implemented to predict storm runoff amount and the peak runoff rate for erosion simulation. The GA infiltration equation was also adopted for erosion prediction in rangeland in RHEM (Nearing *et al.* 2011). In EUROSEM (Morgan *et al.* 1998), the Smith–Parlange infiltration equation (Smith & Parlange 1978) was used for runoff calculation. In LISEM, the Richards equation and Holtan infiltration equation (Holtan 1961; Holtan & Lopez 1971) were options to simulate runoff for erosion modelling (De Roo *et al.* 1996).

doi: 10.2166/nh.2017.003

The Loess Plateau region in China is known worldwide for its high erosion rate and the vast area where extreme rates of erosion occur. With a rugged landscape, deep and erodible loessial soil, the area with severe erosion ($\geq$15,000 t km^{-2} yr^{-1}) is about 36,700 km^2 (MWR 2010; Gao *et al.* 2015). The severe erosion area in the Loess Plateau region is about 89% of the total area of severe erosion in China (MWR 2010; Gao *et al.* 2015). The Loess Plateau region is characterized by a thick loessial layer which is fairly uniform in texture with a large water storage capacity (Zhu 1998). Runoff-producing storms in the region are typically high in intensity and short in duration (Li *et al.* 2009). Infiltration excess is believed to be the main mechanism for runoff generation in this region, and infiltration rates have been extensively measured in the field, mostly with double-ring infiltrometers (Jiang & Huang 1986). Jiang & Huang (1986) summarized typical infiltration capacities for a number of areas in the Loess Plateau region, including a steady-state infiltration capacity ranging from 69 to 78 mm hr^{-1} for the study area considered in this paper.

A number of attempts have been made to evaluate various infiltration equations to describe the measured infiltration rates (e.g. Mishra *et al.* 2003; Zolfaghari *et al.* 2012). For the Loess Plateau region, Wang *et al.* (2004) compared the Kostiakov and Horton infiltration equations using a constant-head infiltrometer under saturated conditions. Mu *et al.* (2008) evaluated the Philip infiltration equation using an indoor rainfall simulator. For runoff and soil loss prediction using process-based models in the Loess Plateau region, Shen (1983) adapted the GA model to simulate runoff for Chabagou (area = 187 km^2), Xiaolihe (area = 802 km^2) and Yeyuhe (area = 282 km^2) catchments. Huang *et al.* (2005) also used the GA model to simulate runoff hydrographs at the hillslope scale. For erosion prediction at the plot-scale in this region, WEPP was used to test model performance for different slope lengths (Wang *et al.* 2007) and slope steepness (Wang *et al.* 2008). At the catchment scale, WEPP was applied to predict annual runoff (Zhang 2004). LISEM was successfully calibrated for a catchment (area = 2 km^2) in the Loess Plateau region (Hessel *et al.* 2003). For a slightly larger catchment of 7.14 km^2, LISEM was used to predict soil erosion for different land use types (Zhang *et al.* 2008).

Parameters to predict runoff hydrographs included effective saturated hydraulic conductivity *Ks*, Manning's *n*, initial suction head and channel length; and they were calibrated to match the peak discharge and total runoff volume. It is noted that separate calibration is needed for each runoff event (Hessel *et al.* 2003). The calibrated *Ks* was found to be in the range of 19.3–22.1 mm hr^{-1} for the Ansai experimental site in the Loess Plateau region (109°19′E; 35°51′N) (Wang *et al.* 2007, 2008). *Ks* values for different land use types were measured with double-ring infiltrometers with values ranging from 4.1 to 14.4 mm·hr^{-1}. Peak runoff rates were found to be underestimated using these measured *Ks* values (Zhang *et al.* 2008). While a number of individual infiltration models have been trialed for different sites and with different data sets, no attempt has been made to systematically compare different infiltration models using the same high-resolution rainfall-runoff data for the Loess Plateau region.

For this study, three different infiltration models of the same level of complexity (each model has two parameters for runoff generation and one for concentration) were calibrated using observed rainfall-runoff data from the Tuanshangou experimental station in the Chabagou catchment. Chabagou is a typical catchment in the Loess Plateau region. Data from this site have been widely used for soil erosion research (e.g. Bao 1995; Liu *et al.* 2000), for quantifying the scale effect on runoff and sediment yield (Fang *et al.* 2008a, 2011) and the effect of rainfall characteristics on runoff and sediment transport (Fang *et al.* 2008b; Zhang *et al.* 2015, 2016). Rainfall and runoff data for selected storm events from the site were also used to test the GA infiltration model (Shen 1983; Huang *et al.* 2005). The three infiltration models tested in this comparative study are: (a) the GA; (b) initial infiltration amount followed by a constant infiltration (CI) rate; (c) initial infiltration amount followed by a variable infiltration (VI) rate. Each of the three infiltration models has two parameters for a fair comparison. The first model has been widely used in process-based erosion prediction models. The second model is arguably the simplest two-parameter infiltration model available; and the CI rate, sometimes known as the ϕ–index, has been used widely for computing excess rainfall (Chow *et al.* 1988). The last model, known as SVIM, is based on the notion of spatially VI capacity, and was developed in conjunction with another process-based erosion model, GUEST (Misra & Rose 1996; Rose *et al.* 2011). Previous research indicated that the performance of SVIM is no worse than the GA

for a number of sites located in tropical and sub-tropical regions of Australia and South-east Asia (Yu 1999). These models, however, have never been comparatively assessed for sites in the Loess Plateau region of China.

The objectives of the study were: (1) to evaluate three different infiltration models to characterize surface runoff processes in the Loess Plateau region; (2) to identify factors or processes that affect model performance; (3) to assess runoff sensitivity to model parameters; (4) to quantify likely errors when these infiltration models were used to predict runoff hydrograph at ungauged events in the region.

DATA AND METHODS

Tuanshangou experimental site selected for this research is located in Chabagou, a typical catchment of 205 km^2, in the northern part of the Loess Plateau region (Figure 1). The soil in the area was fine-loamy, mixed mesic Typic Udorthents, with 46.1% of sand, 48.7% of silt and the rest 5.2% of clay for the upper 10 cm of the soil layer (Liu *et al.* 2000). The rainfall-runoff data used in this study were collected from three plots in Tuanshangou catchment for the period 1963–1967 (Figure 1; Yellow River Water Resource Commission 1966, 1968, 1971). The crops grown on these plots were millet in 1963 and 1967, and potato in 1964 and 1966. The three plots all had a width of 15 m, slope of 40.4%, and lengths of 20, 40 and 60 m, respectively. In effect, the three plots could be regarded as replicates apart from the difference in slope length. All the runoff-producing storm events were considered and analyzed. Rainfall-runoff data were recorded at variable time intervals, with a finer time interval of about 1-min near the peak of storm events. As a result, the original data were linearly interpreted at a fixed 1-min interval for model comparison and evaluation. The 11 largest events in terms of the sediment yield were selected for this study. These events collectively contributed to more than 90% of total sediment yield over the period. As these plots were adjacent to one another, the same rainfall data were used for all three plots (Figure 1 and Table 1), although runoff data at the downslope end of each plot were separately recorded and processed. The volumetric runoff coefficient (average event runoff/average event rainfall) ranged from 36 to 42%, and the ratio of the average peak runoff rate over the average peak rainfall rate varied from 0.61 to 0.74. Plot length, rainfall and runoff characteristics are summarized and presented in Table 1.

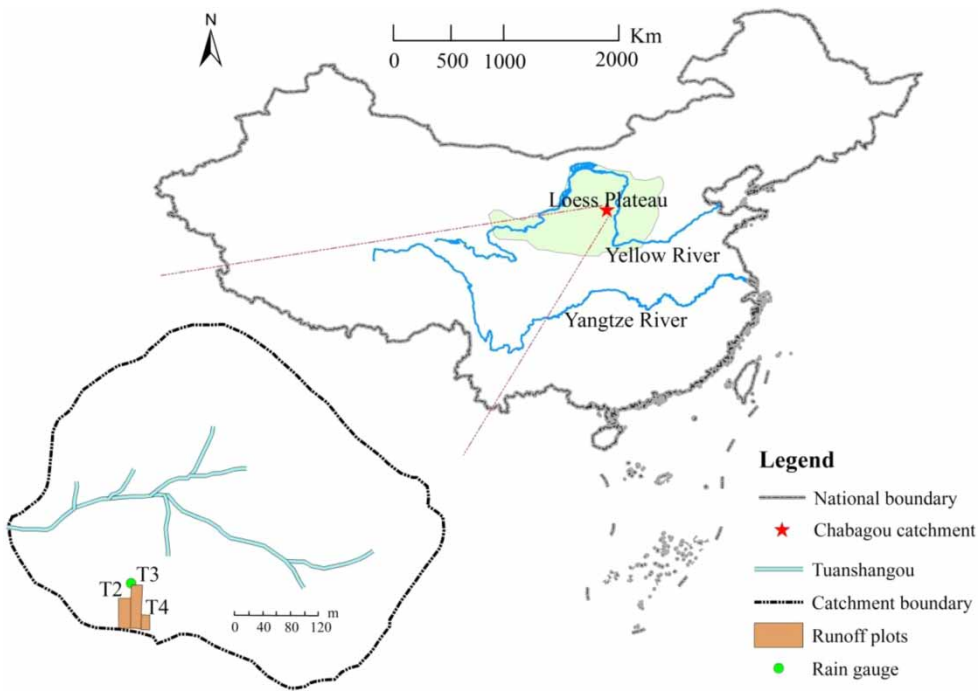

Figure 1 | Location of the study area and experiment plots.

Table 1 | Plot length and runoff characteristics for the 11 largest events

Plot	T4	T2	T3
Length (m)	20	40	60
Average event rainfall amount (mm)	27.6		
Average peak rainfall rate (mm hr^{-1})	134.7		
Average event runoff amount (mm)	9.9	11.5	10.2
Average peak runoff rate (mm hr^{-1})	93.3	99.8	81.5
Contribution to sediment yield from the top 11 events (%)	95	92	93

Infiltration models to be evaluated

CI rate model

An initial infiltration amount, F_o in mm, was assumed. No runoff would occur unless rainfall amount exceeded F_o. A CI capacity, ϕ in mm h^{-1}, was assumed once runoff commenced. Let p_i be the rain rate, e_i be the excess rain rate, both in mm hr^{-1}. For the infiltration model based on a CI rate with parameters F_o and ϕ, the excess rain rate is given by:

$$e_i = 0, \text{ when } \sum_{i=1}^{l} p_i \Delta t < F_o \tag{1}$$

else

$$e_i = \max\{0,\ p_i - \phi\} \tag{2}$$

The summation in Equation (1) represents the cumulative rainfall amount over the first l time intervals. This is one of the most simple methods to compute the excess rain rate. The CI rate parameter, ϕ, is sometimes called the ϕ-index (Chow *et al.* 1988). The CI model, for its simplicity, may be regarded as a baseline case against which other models can be compared.

Spatially VI model

To describe the spatial variability in the infiltration capacity simply, Yu *et al.* (1997b) developed an infiltration model involving two parameters – the initial infiltration amount F_o (identical to that used in CI), and a spatially averaged infiltration capacity, I_m in mm hr^{-1}. An exponential equation was assumed to show the spatial distribution of the infiltration capacity, and excess rain rate could be determined as follows:

$$e_i = p_i - I_m(1 - e^{-p_i/I_m}) \tag{3}$$

Equation (3) shows a non-linear relationship between the rain rate, p_i, and the excess rain rate, e_i. It is also of interest to note that this is irrespective of the magnitude of the spatially averaged infiltration capacity, I_m. The value of e_i computed using Equation (3) is guaranteed to be non-negative.

GA infiltration model

Based on an approximate application of the Darcy's law to describe water movement in an unsaturated soil column (Green & Ampt 1911), the GA equation was adapted to model infiltration under steady rain (Mein & Larson 1973) and unsteady rain (Chu 1978), and was implemented to predict runoff and soil loss in WEPP (Nearing *et al.* 1989; Foster *et al.* 1995). The GA infiltration model in essence has two parameters: *Ks*-effective saturated hydraulic conductivity (mm hr^{-1}) and *Ns*-effective wetting-front matrix potential (mm). The latter is defined as the product of wetting-front matric potential and the soil moisture deficit. In the equation, the basic relationship between the infiltration capacity, f_c in mm, and cumulative infiltration amount, F in mm, is given by:

$$f_c = Ks\left(1 + \frac{Ns}{F}\right) \tag{4}$$

Equation (4) indicates a rapid decrease in the infiltration capacity as the cumulative infiltration amount increases, and f_c would decrease more rapidly with larger *Ns*. For each time interval through a storm event, the rain rate would be compared with f_c to see whether rain excess occurs or not. The incremental infiltration amount, ΔF, is simply $p_i \Delta t$ when rain excess does not occur; otherwise it is given as (Chow *et al.* 1988):

$$\Delta F = Ks\Delta t + Nsln\left(\frac{Ns + F_i + p_i\Delta t}{Ns + F_i}\right) \tag{5}$$

and

$$e_i = p_i - \frac{\Delta F}{\Delta t} \tag{6}$$

where F_i is the cumulative infiltration amount at the end of the previous time interval.

All the three infiltration models, namely CI, VI, GA, have two parameters each. The parameters F_o and Ns control when excess rain, hence runoff, begins, while parameters ϕ, I_m and Ks control the level of infiltration rate through the storm event.

Runoff routing algorithm

The excess rain calculated by the infiltration models needs to be routed to the plot outlet to compare with the observed hydrograph recorded at the downslope end of the each plot. For this study, kinematic wave approximation was used for routing purposes. A linear relationship between the water in store over the plot and the runoff rate at the plot outlet was assumed (Yu *et al.* 1997a; Yu *et al.* 2000), leading to:

$$q_i = \frac{\Delta t}{K + \Delta t} e_i + \frac{K}{K + \Delta t} q_{i-1} \tag{7}$$

where K is the lag time. Thus the runoff rate at the downslope end of the plot can be seen as a weighted sum of the excess rain rate for the current time interval, e_i, and the runoff rate for the previous time interval, q_{i-1}.

The same runoff routing with a single parameter representing the time lag K was implemented for all three runoff plots and for all storm events.

Model calibration and performance indicators

The three infiltration models were calibrated and model parameters for each storm event were estimated by minimizing the sum of squared errors, i.e.:

$$\min \sum_{i=1}^{n} (q_i - \hat{q}_i)^2 \tag{8}$$

where $\hat{q}_i$ is the simulated or modelled runoff rate for time interval i, and n is the total number of 1-min interval for the storm hydrograph. In addition to the storm hydrograph for individual events, the total storm runoff amount (Q in mm), peak runoff rate (Q_p in mm hr^{-1}), and a soil erosion index, Q_s in mm$^{1.4}$ hr$^{-0.4}$ were also considered for infiltration model assessment and comparison. The erosion index was defined as:

$$Q_s = \sum q_i^{1.4} \Delta t \tag{9}$$

as the GUEST framework suggests that the sediment concentration is broadly proportional to $q^{0.4}$ and Q_s is therefore related to the total amount of soil eroded (Yu *et al.* 1997a, 1997b).

The following indicators were used to assess model performance:

(a) Nash–Sutcliffe coefficient (NSC) of efficiency, E_c (Nash & Sutcliffe 1970)

This is an indicator commonly and widely used in model evaluation. E_c is defined as:

$$E_c = 1 - \frac{\sum (O_i - M_i)^2}{\sum (O_i - \bar{O})^2} \tag{10}$$

where O_i represents observations, $\bar{O}$ the mean of observations, and M_i modelled values. E_c ranges from $-\infty$ to 1. The higher the E_c value, the better the model performance. When $E_c = 1$, perfect agreement between predictions and observations is observed; when $E_c = 0$, model predictions are as good as the average observed values.

(b) Bias in model predictions

Bias is defined in this paper as the ratio of the modelled value over the observed value, namely:

$$Bias = \frac{\bar{M}}{\bar{O}} \tag{11}$$

where $\bar{M}$ indicates the mean of modelled values and $\bar{O}$ the mean of observations. The value of Bias >1 indicates overestimation, while Bias <1 indicates underestimation.

(c) Root-mean squared error (*RMSE*)

$$RMSE = \sqrt{\frac{\sum (O_i - M_i)^2}{m1 - m2}} \quad (12)$$

where m_1 and m_2 are the number of observations and the number of parameters, respectively. *RMSE* is dimensional, and quantifies the size of error bars. The mean runoff rate, $\bar{q}$, was used to scale *RMSE* to indicate the size of the error relative to the scale of the problem.

For local sensitivity analysis, the following sensitivity index was computed:

$$Sen = \left| \frac{(y - y_o)/y_o}{(x - x_o)/x_o} \right| \quad (13)$$

where x_o is the calibrated parameter value, and x an adjusted (±10%) parameter value. The change in the parameter value, $\Delta x = x - x_o$ led to a change in model output from y_o to y. The ratio of Δy $(=y - y_o)$ over Δx is an approximation of the partial derivative of the model output with respect to the model parameters, and is commonly used as a straightforward measure of model sensitivity (Saltelli *et al.* 2004). In this paper, the ratio of $\Delta y/y_o$ over $\Delta x/x_o$ was used as a measure of relative sensitivity of predicted runoff to model parameters. For the three infiltration models assessed in this study, parameters are related to the magnitude of infiltration, and runoff would therefore decrease as model parameter values increase. Thus, the ratio of $\Delta y/y_o$ over $\Delta x/x_o$ would be negative in all cases. We thus took the absolute value of the ratio in Equation (13) to indicate how sensitive runoff is to changes in model parameters.

RESULTS

Evaluation of model performance

A summary of four indicators for model performance is presented in Table 2, showing the average model performance in terms of the E_c value for individual runoff hydrographs, and overall bias in terms of runoff amount, the peak runoff rate and the soil erosion index for all 33 plot-events. Overall, the three models performed well when calibrated, with the mean event E_c value in excess of 0.75. The difference in the performance of these infiltration models is small for all three plots, although the results for different treatments show a similar pattern for the three models with better simulation results for T3 (60 m long). In general, VI performed better than CI based on these indicators. Figure 2 shows as an example of the observed and modelled runoff hydrographs for a typical storm event with an E_c value of 0.81 for CI, 0.79 for VI, and 0.76 for GA. Figure 3 shows a comparison in terms of the E_c value between GA and CI, and GA and VI for the 33 plot-events considered. Only six out of the total of 99 E_c values are less than 0.4, with three values as low as zero, which occurred for plot 2 on the 22 August 1967. There may be some data-related issues with this storm event as the observed peak runoff rate (72 mm hr^{-1}) was somehow higher than the observed peak rainfall intensity (66 mm hr^{-1}).

Observed and modelled event total runoff amounts (Q) show a good agreement for all three infiltration models (Figure 4(a)). For CI, 24 of the 33 events (73%) had errors within ±5%. The errors varied in the same range for 20 events (61%) for GA and 15 events (45%) for VI. Overestimation tends to occur for large Q (Figure 4(a)). The average bias was 1.00 for all models and runoff events,

Table 2 | Overall performance indicators for all plot-events and values for three individual plots are given in bracket (T4, T2, T3)

Indicators	CI	VI	GA
E_c_event	0.76 (0.68, 0.72, 0.87)	0.78 (0.75, 0.72, 0.87)	0.76 (0.70, 0.72, 0.86)
Bias_Q	0.97 (0.94, 0.98, 1.00)	1.04 (1.04, 1.03, 1.06)	1.00 (0.98, 1.00, 1.01)
*Bias_*Q_p	0.74 (0.70, 0.68, 0.86)	0.73 (0.71, 0.67, 0.83)	0.74 (0.72, 0.67, 0.84)
*Bias_*Q_s	0.90 (0.88, 0.88, 0.94)	0.94 (0.93, 0.91, 0.97)	0.91 (0.91, 0.89, 0.94)

E_c, Nash–Sutcliffe coefficient of efficiency; *Bias*, ratio of the mean modelled over observed values; CI, constant infiltration rate; VI, variable infiltration rate; GA, Green–Ampt.
The E_c value refers to the mean of E_c for individual runoff hydrographs, while the bias is based on the mean values for all runoff events.

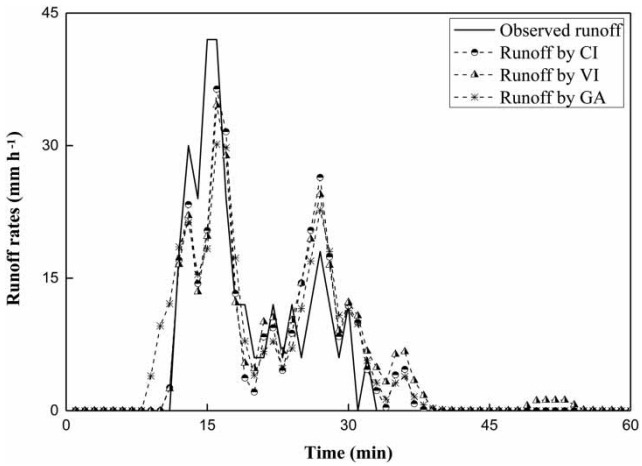

Figure 2 | Observed and modelled hydrographs for a typical storm event (28-Aug-1963) for T2 ($E_c = 0.81$ for CI, 0.79 for VI, and 0.76 for GA).

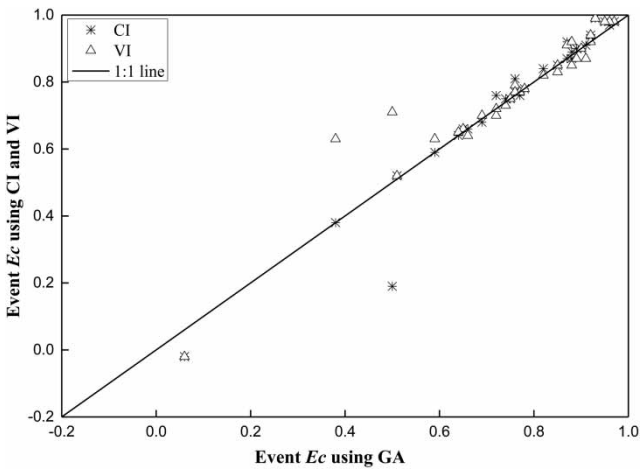

Figure 3 | A comparison of the model efficiency (E_c) for different infiltration models (CI, constant infiltration rate; VI, variable infiltration rate; GA, Green–Ampt).

very close to the slope (1.01) of linear regression through the origin for the runoff amount (Figure 4(a)). The peak runoff rate (Q_p) and the soil erosion index (Q_s) are critical to soil erosion prediction. All three infiltration models did not perform as well, especially with respect to the peak runoff rate. Firstly, the average bias in Q_p was about 0.74, with 77 of all the 99 runoff events (78%) underestimated, and the absolute error increases as Q_p increases. The slope of linear regression through the origin is 0.71 (Figure 4(b)), indicating a systematic underestimation of about 30% for the peak runoff rate. The average bias in Q_s was 0.92, much closer to 1 than that for Q_p, and an underestimation is quite evident for large Q_s with the slope of linear regression through the origin at 0.92 (Figure 4(c)). The pattern for Q_s is opposite to that for Q (Figure 4(c) vs. Figure 4(a)). Overall, VI was associated with slightly higher E_c values and had better bias in terms of Q_s, while GA performed slightly better in terms of Q and Q_p, although the differences among models, especially between VI and GA, seemed to be quite small.

As shown above, the model performance varied from one runoff event to another. Factors that could affect the model performance were considered. To identify model performance for different rainfall-runoff events and to relate model performance to various rainfall-runoff characteristics, the NSC of efficiency and $RMSE/\bar{q}$ were related to the volumetric runoff coefficient (R_c) and the ratio of the peak rainfall intensity and the peak runoff rate, Q_p/P_p, to examine how model performance was affected by rainfall-runoff characteristics (Figure 5). Broadly speaking, the higher the volumetric runoff coefficient (R_c), the smaller the RMSE relative to the mean runoff rate shown as $RMSE/\bar{q}$ (Figure 5(a)) and the NSC of efficiency increases with the ratio of the peak runoff rate over the peak rainfall intensity (Figure 5(b)). In other words, the model performance deteriorates when the hydrological response is weak and relatively little runoff was generated.

Assessment of model parameters

The three infiltration models evaluated in this study are of the same degree of complexity with two parameters each, with the lag time in the routing component, K, common to all three models, the initial infiltration amount before runoff occurs, F_o, for CI and VI, and the other parameters all related to infiltration rates. A summary of the mean and 1-standard deviation of the nine model parameters is shown in Table 3. Table 3 shows that there are differences in the mean of calibrated parameter values for K and F_o, although their values are expected to be identical for the same plot. There are also variations in the mean of the calibrated parameter values among the three different plots. The infiltration parameter values, i.e. ϕ, I_m, Ks are generally lower for T2 in comparison with the other two plots, which was clearly related to the higher runoff amount for this plot in comparison with the other two (Table 1).

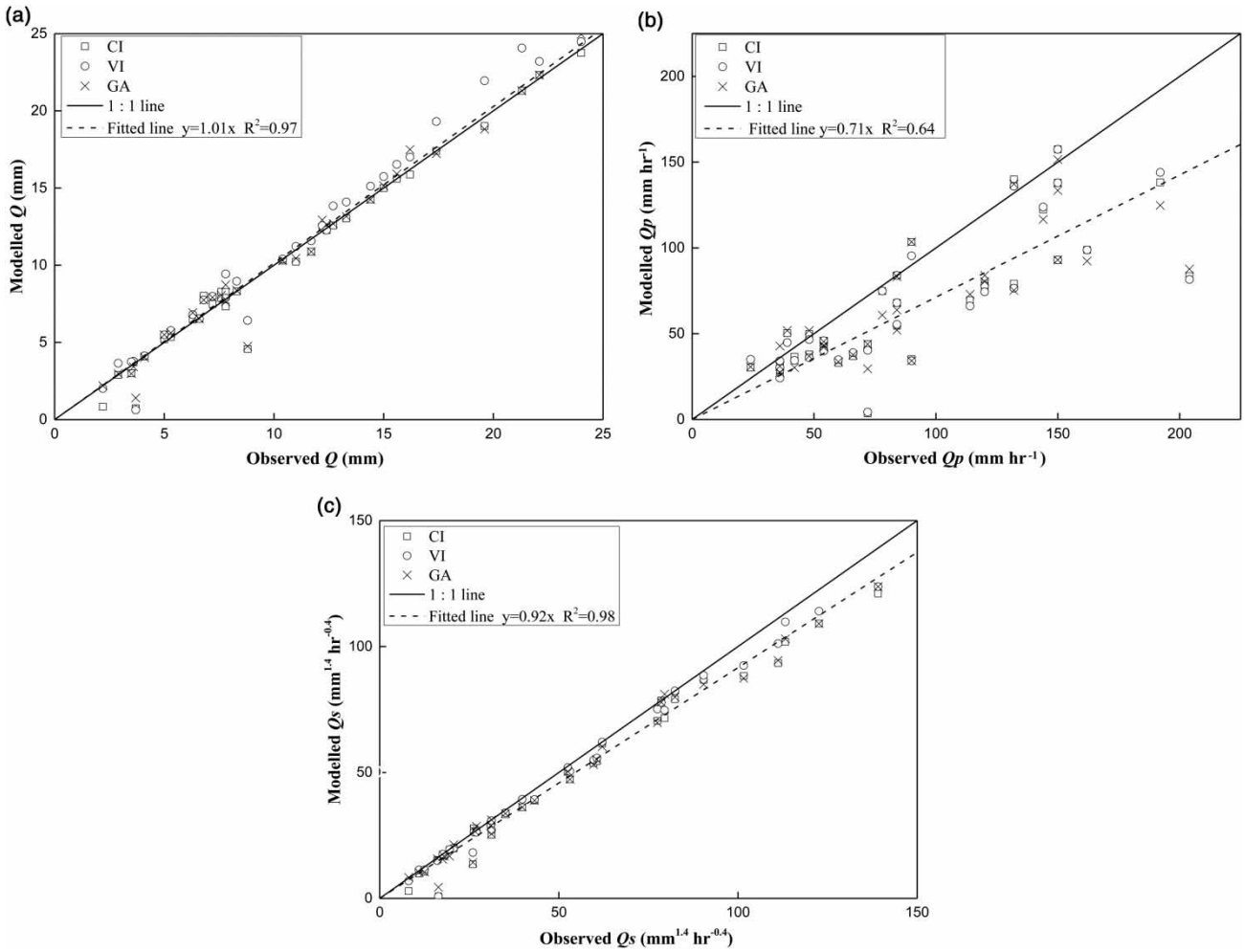

Figure 4 | Comparisons of observed and estimated runoff amount (a), peak runoff rate (b), and the soil erosion index (c) using calibrated parameter values for individual storm events.

Calibrated model parameter values were compared with those that could be determined directly from analyzing the observed rainfall and runoff data. Different methods of determining the lag time were described in previous research (Watt & Chow 1985; Aron *et al.* 1991; Loukas & Quick 1996). The lag time may be simply determined as the time difference between the peak runoff rate recorded at the plot outlet and the peak rainfall intensity (Yu *et al.* 2000). For comparison purposes, the lag time based on the peak rainfall and runoff was designated as *Kp*. The computed mean value for *Kp* was 1.4 min for T4 (20 m long), 1.9 min for T2 (40 m long) and 1.2 min for T3 (60 m long) (Table 3). The computed lag time was in good agreement with the lag time calibrated with the VI model and the simple routing algorithm (Table 3), although the lag time determined in this way was not proportional to the slope length as expected. Another parameter, F_o, for CI and VI may also be determined from the rainfall-runoff data without having to calibrate the infiltration models. From its definition, F_o could be determined by adding up all the rainfall that occurred prior to commencement of runoff (denoted as F_o'). Similar to *Kp*, F_o' was estimated to be 6.1 mm for T4, 6.7 mm for T2, and 6.4 mm for T3 using the observed rainfall and runoff data. These F_o' values are about 20% higher than those calibrated initial infiltration amounts for VI and 35% higher for CI (Table 3). The parameters of the GA infiltration equation cannot be determined from the rainfall-runoff observations without calibration.

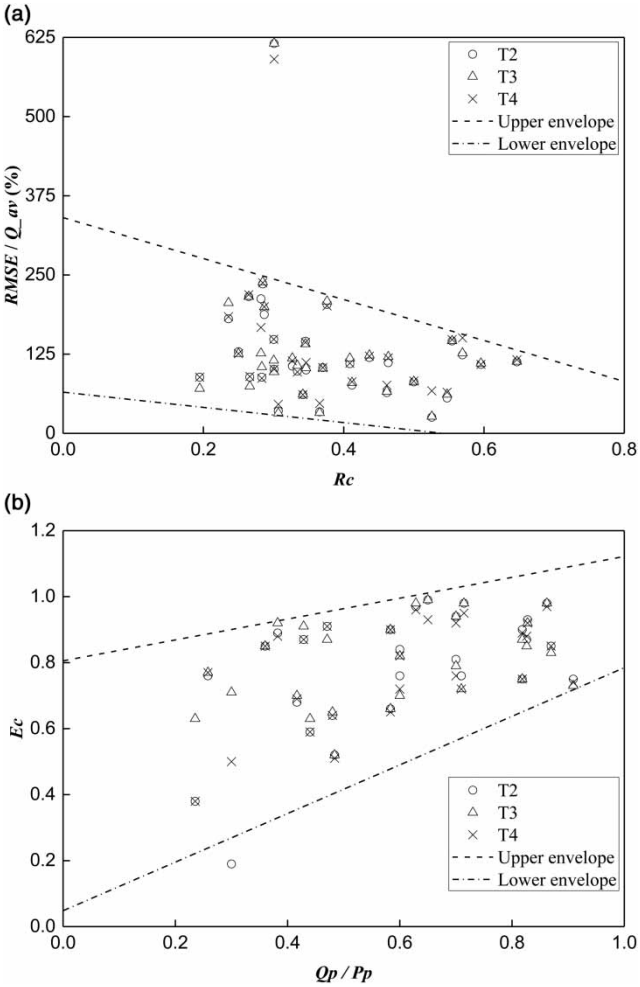

Figure 5 | The relationship between the volumetric runoff coefficient (R_c) and the RMSE/$\bar{q}$ (a) and the ratio of the peak runoff rate over peak rainfall rate (Q_p/P_p) and the Nash–Sutcliffe coefficient of efficiency (E_c) (b).

As the infiltration models were calibrated and parameters were estimated for individual runoff events, parameter variability was examined and models for which parameters do not vary a great deal would be easier to use. Figure 6 shows the distributions of the nine parameters for the three infiltration models based on the 33 events. The calibrated parameter values were all standardized by the mean for comparing the variability of these parameters, as the ratio of the calibrated parameter for individual event over the mean for all events is non-dimensional. The smaller the range in this ratio is, the lower the variability for the parameter, and the easier for model application. For comparison, some of the parameters are plotted next to one another as they are similar in nature. Additional information is provided on the standard deviation for each of the nine parameters for each of the three plots (Table 3). Based on the size of the box plot in Figure 6, infiltration parameters for CI and VI have a similar degree of variability with the ratio of the 3rd quantile over the 1st quantile for the parameters ranging from 2.10 for F_o in VI to 2.97 for I_m. The variability of the GA parameters was much higher; the quantile ratio for *Ks* was 3.45, and as high as 245 for *Ns* (see also Figure 6). The quantile ratio for the lag time varied from 2.85 for VI to 4.06 for CI.

In addition to parameter variability, sensitivity analysis indicates quite different runoff response to changes in parameter values. Figure 7 shows how the runoff amount changes as a result of a 10% decrease and 10% increase in each of the six calibrated parameters. In general, the

Table 3 | Calibrated parameter values (the mean ± standard deviation) for the three infiltration models evaluated

Model	Parameter	T4	T2	T3	All three plots
CI	F_o (mm)	4.7 ± 4.0	5.5 ± 3.6	4.2 ± 1.7	4.8 ± 3.2
	ϕ (mm hr^{-1})	33.8 ± 13.3	26.3 ± 16.7	32.1 ± 26.0	30.8 ± 19.1
	K (min)	2.1 ± 2.8	2.6 ± 2.3	1.4 ± 1.2	2.0 ± 2.2
VI	F_o (mm)	5.0 ± 4.5	6.1 ± 3.5	5.1 ± 4.1	5.4 ± 3.9
	I_m (mm hr^{-1})	45.6 ± 25.4	37.0 ± 27.5	44.6 ± 39.6	42.4 ± 30.7
	K (min)	1.6 ± 2.0	1.9 ± 1.8	1.3 ± 0.9	1.6 ± 1.6
GA	*Ks* (mm hr^{-1})	23.4 ± 15.9	18.6 ± 12.9	25.6 ± 25.8	22.5 ± 18.7
	Ns (mm)	34.8 ± 64.1	17.6 ± 25.6	52.3 ± 156.2	34.9 ± 96.5
	K (min)	2.0 ± 2.5	2.1 ± 1.9	1.4 ± 0.9	1.8 ± 1.8
Through model calibration	Average K (min)	1.9 ± 2.4	2.2 ± 2.0	1.3 ± 1.0	1.8 ± 1.9
Through data analysis	*Kp* (min)	1.4 ± 3.9	1.9 ± 3.9	1.2 ± 3.5	1.5 ± 3.7
Through model calibration (CI and VI)	Average F_o (mm)	4.9 ± 4.2	5.8 ± 3.5	4.6 ± 3.1	5.1 ± 3.6
Through data analysis	Average F_o' (mm)	6.1 ± 4.4	6.7 ± 4.3	6.4 ± 4.4	6.4 ± 4.3

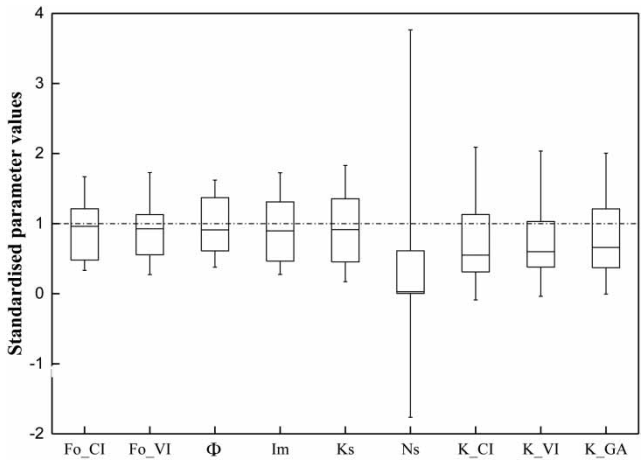

Figure 6 | Variability of model parameters: Range: 25–75%; Whisker: 1 standard deviation; Line – the median. Parameter values have been standardized by the mean.

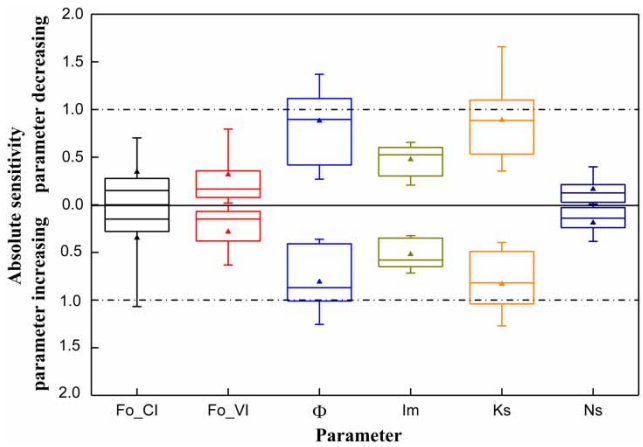

Figure 7 | Sensitivity of total runoff amount (Q) to changes (decrease by 10% and increase by 10%) of model parameter values; Range 25–75%, Whisker (10–90%), the line in the middle indicates the median, and the symbol the mean.

runoff amount is more sensitive to changes in ϕ, I_m and Ks than to F_o and Ns (Figure 7). Of the three sensitive parameters, the runoff amount is less sensitive to I_m than to ϕ and Ks. The absolute sensitivity for parameters for VI is all less than unity, with an average of 0.5, for all the 33 plot-events tested, indicating that the relative error in predicted runoff amount is on average half of that in the parameter values. For CI, a 10% change in ϕ would result in an 8.5% change in the modelled runoff amount; and for GA, a 10% change in Ks would result in an 8.6% change in runoff on average. Finally it is also interesting to note that the absolute sensitivity is almost symmetric with respect to ±10% changes in model parameters. Sensitivity analysis of the peak runoff rate (Figure 8) shows that the peak runoff rate is much less sensitive to model parameters than the runoff amount (c.f. Figures 7 and 8). Broadly speaking, the relative sensitivity for the peak runoff rate is about half of that for the runoff amount. The initial infiltration amount, F_o, has minimal effect on the simulated peak runoff rate (Figure 8). In terms of the three parameters ϕ, I_m and Ks, again the peak runoff rate is least sensitive to the parameter I_m in VI (Figure 8).

In summary, parameter values for VI are closer to those calculated directly from rainfall-runoff data (Kp and F_o'), and overall they are less variable and sensitive when predicting event runoff amount and the peak runoff rate in comparison to the other two models.

Runoff prediction using average parameter values

As the three infiltration models and all their parameters were calibrated for individual events, both model performance and the calibrated parameter values varied widely from event to event (Figure 3 and Table 3). In view of the large parameter variability and a lack of an effective means to calculate parameters for individual events, the average parameter values for all events of each site were used to predict runoff hydrographs as if these were ungauged events to test how well the models would perform in terms of simulated runoff hydrographs. The same model

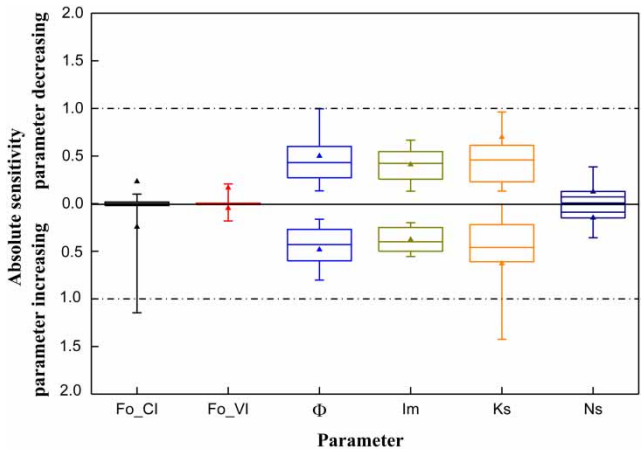

Figure 8 | Sensitivity of the peak runoff rate (Q_p) to changes (decrease by 10% and increase by 10%) of parameter values; Range 25–75%, Whisker (10–90%), the line in the middle indicates the median, and the symbol the mean.

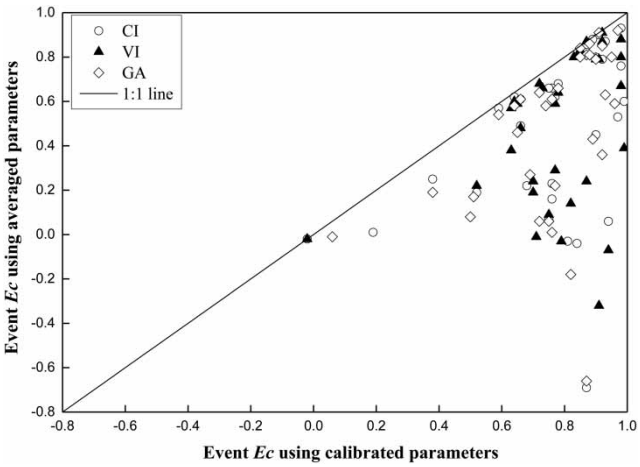

Figure 9 | Comparison of model efficiency (E_c) with calibrated and average parameter values.

performance indicators were applied to the predicted runoff hydrographs using the average parameter values. As expected, the event (E_c) value shows a noticeable reduction when the hydrograph was predicted using this set of constant parameter values (Figure 9). It is clear that the model performance deteriorated considerably, and the mean of (E_c) decreased from 0.76 to 0.47, having used the average parameter values for the 33 plot-events. Figure 10 shows the difference in model output, i.e. Q, Q_p and Q_s, separately using calibrated and averaged parameters for all the events and for all three infiltration models. Table 4 presents the NSC of efficiency, the bias, and the root-mean-square-error for runoff amount, the peak runoff rate and the erosion index for the three different infiltration models. While the (E_c) values for all items decreased a great deal for the

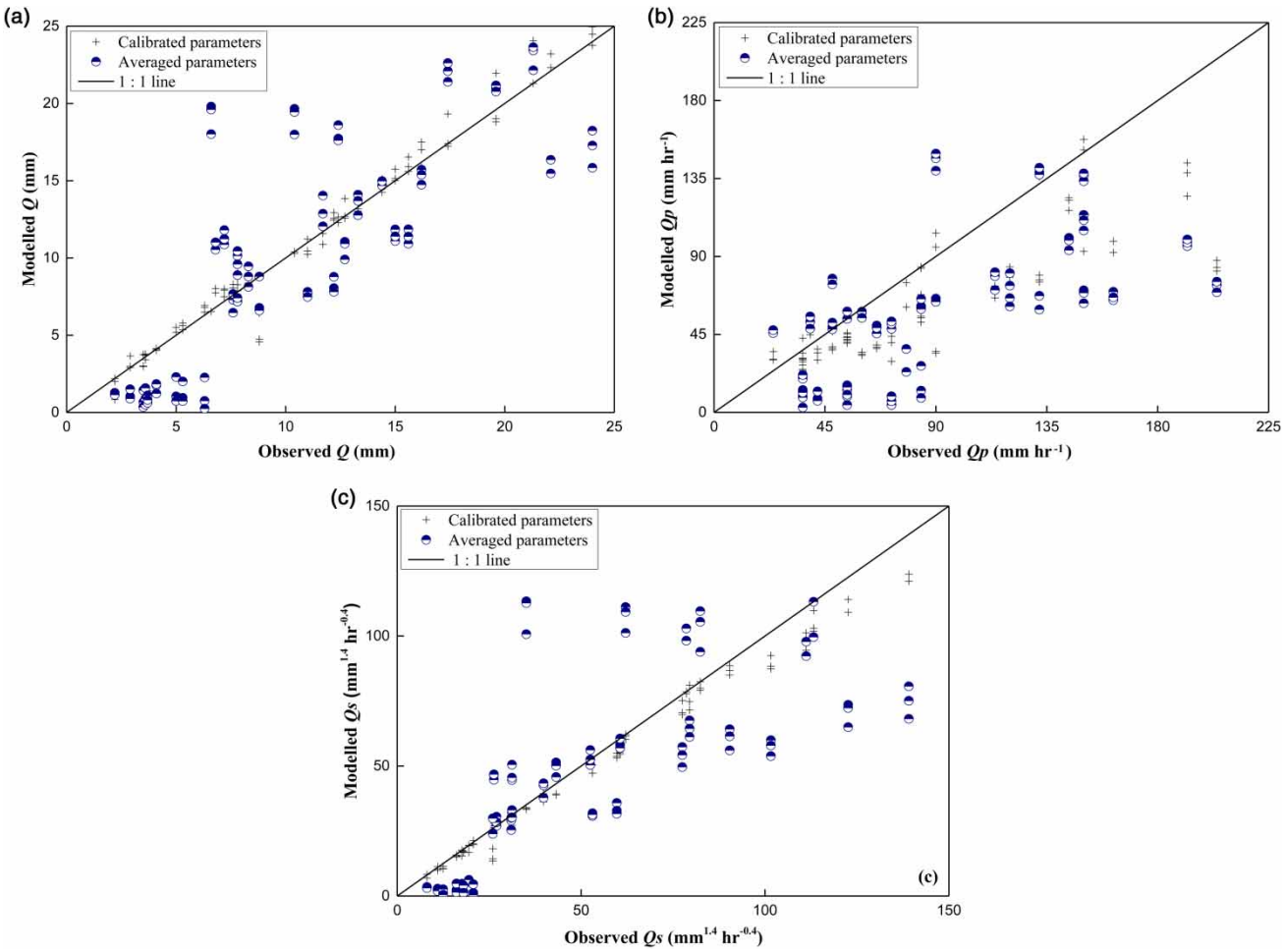

Figure 10 | Comparison of model performance between results of calibrated and averaged parameter values for runoff amount (a), peak runoff rate (b) and the soil erosion index (c).

Table 4 | Comparison of model efficiency (E_c), *Bias* and *RMSE* for runoff amount (Q), peak runoff rate (Q_p), and the soil erosion index (Q_s) using calibrated and averaged parameter values

Models	CI		VI		GA	
Variable	Cal[a]	Ave[b]	Cal[a]	Ave[b]	Cal[a]	Ave[b]
E_c_Q	0.97	0.48	0.96	0.54	0.97	0.46
$E_c\_Q_p$	0.40	–0.04	0.39	–0.14	0.40	–0.05
$E_c\_Q_s$	0.96	0.48	0.98	0.47	0.96	0.45
$Bias\_Q$	0.97	0.97	1.04	0.97	1.00	0.95
$Bias\_Q_p$	0.74	0.66	0.73	0.63	0.74	0.66
$Bias\_Q_s$	0.90	0.90	0.94	0.85	0.91	0.88
$RMSE\_Q$ (mm)	1.02	4.29	1.18	4.05	0.97	4.39
$RMSE\_Q_p$ (mm hr^{-1})	37.80	49.73	38.13	51.56	45.92	49.99
$RMSE\_Q_s$ ($mm^{1.4}$ $hr^{-0.4}$)	7.67	26.34	5.41	26.73	7.04	27.24

RMSE, Root-mean squared error. [a]Using calibrated parameter values; [b]using average parameter values.

three infiltration models, the changes in the bias were small, varying within 13%. The *RMSE* for the total runoff was increased by a factor between three and five using the average parameter values. The change in *RMSE* for the peak runoff rate was small (<40%) because the *RMSE* values were quite large even using the calibrated parameter values in the first place.

In terms of predicting event total runoff amount (Q), VI is marginally better than CI and GA for the 33 plot-events considered. CI and GA performed slightly better than VI in terms of the peak runoff rate (Q_p), and CI is slightly better than VI and GA in terms of the erosion index.

DISCUSSION

For a comparison of the three infiltration models, one is tempted to rank them and make a choice for implementation for runoff and erosion prediction models. As shown in the Results section, the three models tested were quite similar in performance, and all three models performed less satisfactorily when used to predict runoff hydrographs with the average parameter values. Of the three models evaluated, the VI model has the advantage over the other two because its parameters are least sensitive. In addition, runoff prediction was quite sensitive to GA parameters, and GA parameter values varied more than those for the other two models for the 33 plot-events tested.

One intriguing question to ask is why the peak runoff rate has been systematically underestimated for all three models, while this systematic discrepancy was not noted in previous studies (e.g. Yu *et al.* 1997b; Yu 1999). The noticeable differences include a much steeper slope and high runoff coefficients for the 33 plot-events considered. Perhaps due to concentration of overland flows on steep slopes, the assumed linear storage-discharge relationship may be no longer adequate for runoff routing purposes for this hydrologically responsive and topographically steep regions. If the lag time is much reduced during time intervals of high rain excess rate, a high runoff rate is implied with an increased weight associated with the rain excess term in Equation (7). This is clearly an area for further investigation. In addition, issues with data quality could not be excluded, although the same data set has been extensively used for model testing and development (e.g. Bao 1995; Huang *et al.* 2005; Fang *et al.* 2008a, 2008b, 2011; Zhang *et al.* 2015, 2016; Cheng *et al.* 2016). The peak rainfall was directly recorded at high time resolutions (1 min for the majority) using a self-recording rain gauge (Yellow River Water Resource Commission 1966, 1968, 1971). Linear interpolation was applied only when the time intervals were more than 1-min during periods of low rainfall intensity. This type of rainfall data would normally require siphon and time correction, although how the correction was applied was not clearly described (Yellow River Water Resource Commission 1966, 1968, 1971). The recorded rainfall intensity, especially the high rainfall intensity, could be less than the actual intensity for this type of self-recording rain gauges. The possibility that the measured peak rainfall intensity could be less than the actual peak intensity for the experimental site may have led to an underestimation of the peak runoff rates for most events.

CONCLUSIONS

Based on rainfall-runoff data at 1-min interval for 33 plot-events in Tuanshangou experimental station, three infiltration models of the same degree of complexity with three

parameters each were compared and evaluated. The results showed that all the three models, namely CI rate, spatially VI rate, and GA performed similarly when calibrated for individual storm events with the NSC of efficiency around 0.76. All three models generally performed better for large storm events with higher runoff coefficient. For all three models, the modelled peak runoff rate was systematically smaller by about 30% than the observed peak runoff rate. The calibrated parameter values varied from event to event. The amount of variation in the initial infiltration amount, F_o, is smaller than that in other infiltration parameters, i.e. ϕ, I_m, Ks. Predicted event total runoff amount and peak runoff rates were particularly sensitive to these three parameters. For application at ungauged events, averaged parameter values were used to predict runoff hydrographs for these 33 plot-events, and the results showed a decrease in model performance with an average NSC of efficiency reduced to 0.47. One distinct advantage in using the spatially VI model is that the simulated runoff is least sensitive to variations in model parameters in comparison to the other two models assessed in this study.

ACKNOWLEDGEMENTS

The research was funded by State Key Laboratory of Earth Science Processes and Resources Ecology, Beijing Normal University (No. 2015-KF-10).

REFERENCES

Aron, G., Ball, J. E. & Smith, T. A. 1991 Fractal concept used in time–of–concentration estimates. *J. Irrig. Drain. Eng.* **117** (5), 635–641.

Bao, W. 1995 A conceptual flow–sedimentation coupled simulation model for small basins. *Geogr. Res.* **14** (2), 27–34 (in Chinese).

Cheng, Z., Yu, B. & Fu, S. 2016 An assessment of runoff process-based models for plots in China Loess Plateau. *Sci. Soil Water Conserv.* **14** (6), 10–17 (in Chinese).

Chow, V. T., Maidment, D. R. & Mayes, L. W. 1988 *Applied Hydrology*. McGraw–Hill, New York.

Chu, T. C. 1978 Infiltration during an unsteady rain. *Water Resour. Res.* **14** (3), 461–466.

De Roo, A. P. J., Wesseling, C. G. & & Ritsema, C. J. 1996 LISEM: A single event physically based hydrological and soil erosion model for drainage basins. I: theory, input and output. *Hydrol. Process.* **10** (8), 1107–1117.

Fang, H., Cai, Q., Chen, H. & Li, Q. 2008a Effect of rainfall regime and slope on runoff in a gullied Loess Region on the Loess Plateau in China. *Environ. Manage.* **42** (3), 402–411.

Fang, H., Chen, H., Cai, Q. & Huang, X. 2008b Effect of spatial scale on suspended sediment concentration in flood season in hilly Loess Region on the Loess Plateau in China. *Environ. Geol.* **54** (6), 1261–1269.

Fang, H., Li, Q., Cai, Q. & Liao, Y. 2011 Spatial scale dependence of sediment dynamics in a gullied rolling loess region on the Loess Plateau in China. *Environ. Earth Sci.* **64** (3), 693–705.

Foster, G. R., Flanagan, D. C., Nearing, M. A., Lane, L. J., Risse, L. M. & Finkner, S. C. 1995 Hillslope erosion component, Ch.11. In: *USDA Water Erosion Prediction Project: Hillslope Profile Model Documentation. NSERL Report No. 2* (L. J. Lane & M. A. Nearing, eds). National Soil Erosion Laboratory, USDA–ARS, West Lafayette, IN, USA.

Gao, H., Li, Z., Li, P., Jia, L., Xu, G. & Ren, Z. 2015 The capacity of soil loss control in the Loess Plateau based on soil erosion control degree. *Acta Geogr. Sin.* **70** (9), 1503–1515 (in Chinese).

Green, W. H. & Ampt, G. A. 1911 Studies on soil physics. Part 1: the flow of air and water through soils. *J. Agr. Sci.* **4** (1), 1–24.

Hessel, R., Jetten, V., Liu, B., Zhang, Y. & Stolte, J. 2003 Calibration of the LISEM model for a small Loess Plateau catchment. *Catena* **54** (1), 235–254.

Holtan, H. N. 1961 A concept for infiltration estimates in watershed engineering. USDA-ARS Bulletin 41-51, Washington, DC, 25 pp.

Holtan, H. N. & Lopez, N. C. 1971 *USDAHL-70 Model of Watershed Hydrology. USDA-ARS Tech. Bull. No. 1435.* Agricultural Research Station, Beltsville, MD.

Huang, X., Wang, Z. & Tian, F. 2005 Hydrological model of uniform hillslope in Loess Region. *Bull. Soil Water Conserv.* **25** (6), 45–49 (in Chinese).

Jiang, D. & Huang, G. 1986 Study on the infiltration rate of soil on the Loess Plateau of China. *Acta Pedol. Sin.* **4**, 299–305 (in Chinese).

Li, T., Wang, G., Huang, Y. & Fu, X. 2009 Modeling the process of hillslope soil erosion in the Loess Plateau. *J. Environ. Inform.* **14** (1), 1–10.

Liu, B., Nearing, M. A., Shi, P. & Jia, Z. 2000 Slope length effects on soil loss for steep slopes. *Soil Sci. Soc. Am. J.* **64** (5), 1759–1763.

Loukas, A. & Quick, M. C. 1996 Physically-based estimation of lag time for forested mountainous watersheds. *Hydrol. Sci. J.* **41** (1), 1–19.

Mein, R. G. & Larson, C. L. 1973 Modeling infiltration during a steady rain. *Water Resour. Res.* **9** (2), 384–394.

Mishra, S. K., Tyagi, J. V. & Singh, V. P. 2003 Comparison of infiltration models. *Hydrol. Process.* **17** (13), 2629–2652.

Misra, R. K. & Rose, C. W. 1996 Application and sensitivity analysis of process-based erosion model GUEST. *Eur. J. Soil Sci.* **47** (4), 593–604.

Morgan, R. P. C., Quinton, J. N., Smith, R. E., Govers, G., Poesen, J. W. A., Auerswald, K., Chisci, G., Torri, D. & Styczen, M. E. 1998 The European soil erosion model (EUROSEM): a dynamic approach for predicting sediment transport from fields and small catchments. *Earth Surf. Process. Landforms* **23** (6), 527–544.

Mu, T., Wang, Q. & Wang, H. 2008 Surface runoff formation model based on Philip equation. *J. Soil Water Conserv.* **22** (4), 62–64 (in Chinese).

MWR (Ministry of Water Resources of the People's Republic of China, Chinese Academy of Sciences, Chinese Academy of Engineering) 2010 *Water Loss and Soil Erosion and Ecological Security of China: The Loess Plateau*. Science Press, Beijing, pp. 28–59.

Nash, J. E. & Sutcliffe, J. V. 1970 River flow forecasting through conceptual models, part 1: a discussion of principles. *J. Hydrol.* **10** (3), 282–290.

Nearing, M. A., Foster, G. R., Lane, L. J. & Finkner, S. C. 1989 A process–based soil erosion model for USDA–Water erosion prediction project technology. *Trans. ASAE* **32** (5), 1587–1593.

Nearing, M. A., Wei, H., Stone, J. J., Pierson, F. B., Spaeth, K. E., Weltz, M. A., Flanagan, D. C. & Hernandez, M. 2011 A rangeland hydrology and erosion model. *Trans. ASABE* **54** (3), 901–908.

Rose, C. W., Yu, B., Misra, R. K., Coughlan, K. & Fentie, B. 2011 Use of GUEST technology to parameterize a physically-based model for assessing soil erodibility and evaluating conservation practices in tropical steeplands. In: *Handbook of Erosion Modelling,* 1st edn (R. P. C. Morgan & M. A. Nearing, eds). Blackwell Publishing Ltd, Chichester, UK, pp. 195–222.

Saltelli, A., Tarantola, S., Campolongo, F. & Ratto, M. 2004 *Sensitivity Analysis in Practice: A Guide to Assessing Scientific Models.* Halsted Press, New York.

Shen, B. 1983 The runoff yield calculation model of the loess hilly areas. *J. Shaanxi Inst. Mech. Eng.* **2**, 13–30 (in Chinese).

Smith, R. E. & Parlange, J. 1978 A parameter-efficient hydrologic infiltration model. *Water Resour. Res.* **14** (3), 533–538.

Wang, J., Wu, Q., Han, B. & Dai, X. 2004 Distribution law on infiltration of Loess Hilly Region. *Syst. Sci. Comp. Stud. Agr.* **20** (4), 288–290 (in Chinese).

Wang, J., Zheng, F., Jiang, Z. S. & Zhang, X. 2007 Assessment of WEPP model applicability (hillslope version) on hill–gully region of the Loess Plateau – a case study in slope length factor. *Bull. Soil Water Conserv.* **27** (2), 50–55 (in Chinese).

Wang, J., Zheng, F., Jiang, Z. & Zhang, X. 2008 Assessment on WEPP model applicability (hillslope version) to hill–gully region of the Loess Plateau – a case study in slope gradient factor. *J. Sediment Res.* **29** (6), 52–60 (in Chinese).

Watt, W. E. & Chow, K. A. 1985 A general expression for basin lag time. *Can. J. Civil Eng.* **12** (2), 294–300.

Wischmeier, W. H. & Smith, D. D. 1978 *Predicting Rainfall Erosion Losses: A Guide to Conservation Planning. Agricultural Handbook No.537.* USDA, Washington, DC.

Yellow River Water Resource Commission 1966 *Hydrographic Experiment Data of the Runoff Experimental Establishment of Zizhou in the Yellow River Watershed (1963–1964).* Yellow River Water Resource Commission, Zhengzhou, China.

Yellow River Water Resource Commission 1968 *Hydrographic Experiment Data of the Runoff Experimental Establishment of Zizhou in the Yellow River Watershed (1965–1966).* Yellow River Water Resource Commission, Zhengzhou, China.

Yellow River Water Resource Commission 1971 *Hydrographic Experiment Data of the Runoff Experimental Establishment of Zizhou in the Yellow River Watershed (1967–1969).* Yellow River Water Resource Commission, Zhengzhou, China.

Yu, B. 1999 A comparison of the Green–Ampt and a spatially variable infiltration model for natural storm events. *Trans. ASAE* **42** (1), 89–98.

Yu, B., Rose, C. W., Ciesiolka, C. C. A., Coughlan, K. J. & Fentie, B. 1997a Toward a framework for runoff and soil loss prediction using GUEST technology. *Aust. J. Soil Res.* **35** (5), 1191–1212.

Yu, B., Rose, C. W., Coughlan, K. J. & Fentie, B. 1997b Plot-scale rainfall–runoff characteristics and modeling at six sites in Australia and south east Asia. *Trans. ASAE* **40** (5), 1295–1303.

Yu, B., Rose, C. W., Ciesiolka, C. C. A. & Cakurs, U. 2000 The relationship between runoff rate and lag time and the effects of surface treatments at the plot scale. *Hydrol. Sci. J.* **45** (5), 709–726.

Zhang, X. 2004 Calibration, refinement, and application of the WEPP model for simulating climatic impact on wheat production. *Trans. ASAE* **47** (4), 1075–1085.

Zhang, X., Zhang, S., Cai, D., Zhang, Y. & Sun, X. 2008 Interaction between land use and soil erosion in west Loess Plateau. *J. Lanzhou Uni.* **44** (2), 9–14 (in Chinese).

Zhang, L., Li, Z. & Wang, S. 2015 Impact of runoff regimes on sediment yield and sediment flow behavior at slope scale. *Trans. CSAE* **31** (20), 124–131 (in Chinese).

Zhang, L., Li, Z., Wang, H. & Xiao, J. 2016 Influence of intra-event-based flood regime on sediment flow behavior from a typical agro-catchment of the Chinese Loess Plateau. *J. Hydrol.* **538**, 71–81.

Zhu, X. 1998 The 28-character strategy for reclaiming the Loess Plateau, its theory & practice. *Bull. Chin. Acad. Sci.* **3**, 232–236 (in Chinese).

Zolfaghari, A. A., Mirzaee, S. & Gorji, M. 2012 Comparison of different models for estimating cumulative infiltration. *Int. J. Soil Sci.* **7** (3), 108–115.

First received 15 December 2016; accepted in revised form 21 August 2017. Available online 8 November 2017